Crystallization of Poly(butylene terephthalate)/ Poly(ethylene octene) Blends: Isothermal Crystallization

Jiann-Wen Huang,[1] Ya-Lan Wen,[2,3] Chiun-Chia Kang,[4] Mou-Yung Yeh,[5,6] Shaw-Bing Wen[3]

[1]*Department of Styling and Cosmetology, Tainan University of Technology, Yung Kang City, Taiwan, Republic of China*
[2]*Department of Nursing, Meiho Institute of Technology, Neipu Hsiang, Pingtung, Taiwan, Republic of China*
[3]*Department of Resources Engineering, National Cheng Kung University, Tainan City, Taiwan, Republic of China*
[4]*R&D Center, Hi-End Polymer Film Co., Ltd., 15-1 Sin Jhong Rd., Sin Ying City 730, Taiwan, Republic of China*
[5]*Department of Chemistry, National Cheng Kung University, Tainan City, Taiwan, Republic of China*
[6]*Sustainable Environment Research Centre, National Cheng Kung University, Tainan City 709, Taiwan, Republic of China*

Received 7 March 2007; accepted 6 November 2007
DOI 10.1002/app.27628
Published online 21 May 2008 in Wiley InterScience (www.interscience.wiley.com).

ABSTRACT: Poly(ethylene-octene) (POE), maleic anhydride grafted poly(ethylene-octene) (mPOE), and a mixture of POE and mPOE were added to poly(butylene terephthalate) (PBT) to prepare PBT/POE, PBT/mPOE, and PBT/mPOE/POE blends by a twin-screw extruder. Observation by scanning electron microscopy revealed improved compatibility between PBT and POE in the presence of maleic anhydride groups. The melting behavior and isothermal crystallization kinetics of the blends were studied by wide-angle X-ray diffraction and differential scanning calorimeter; the kinetics data was delineated by kinetic models. The addition of POE or mPOE did not affect the melting behavior of PBT in samples quenched in water after blending in an extrude. Subsequent DSC scans of isothermally crystallized PBT and PBT blends exhibited two melting endotherms (T_{mI} and T_{mII}). T_{mI} was the fusion of the crystals grown by normal primary crystallization and T_{mII} was the melting peak of the most perfect crystals after reorganization. The dispersed second phase hindered the crystallization; on the other hand, the well dispersed phases with smaller size enhanced crystallization because of higher nucleation density. © 2008 Wiley Periodicals, Inc. J Appl Polym Sci 109: 3070–3079, 2008

Key words: blends; crystallization; kinetics; elastomers; melt

INTRODUCTION

Polymer blending is a commonly used technique to improve properties of polymers. Most polymers are, however, immiscible and polymer blends generally involve two-phase. Immiscible polymer blends usually exhibit poor mechanical properties because the incompatibility causes an unstable morphology and poor interfacial adhesion. To obtain high performance materials, the compatibility of the blend has to be achieved.

Poly(butylene terephthalate) (PBT) is an important thermoplastic material for a large number of applications because of its good combination of properties, such as rigidity and solvent resistance. Its low impact strength can be overcome by blending with elastomers, such as poly(ethylene-octene) (POE),[1–3] poly(acrylonitrile-*co*-butadiene-*co*-styrene) (ABS),[4,5] ethylene–propylene–diene (EPDM),[6] ethylene-propylene rubber,[7] and poly(ethylene-*co*-glycidyl methacrylate).[8] Compatibility between PBT and the rubbery phase is an important factor for a tough blend.[1–8] A super-tough PBT blend has been obtained by blending PBT with PEO grafted with maleic anhydride (mPEO) because of good compatibility between PBT and mPEO.[1]

The compatibility of an elastomer with PBT affects not only the mechanical properties, but also the crystallization kinetics of the blend. Toughness of the blend is generally improved with amounts of rubbery phase, while at the same time, rigidity drops.[1] It has been shown that blends of PBT with other polymers may not affect the melting process,[1] but induce drastic changes in the crystallization behavior of PBT.[9–12]

In this article, blends of PBT with POE or mPOE of different compositions were studied. The dispersion was observed by a scanning electron microscope (SEC). The melting and crystallization behavior of PBT in the blends were explored by wide-angle X-ray diffraction (WAXD) and differential scanning calorimeter (DSC). The crystallization kinetics of PBT was simulated by Avrami and Hoffman–Lauritzen models.

EXPERIMENTAL

Materials

Commercial grade PBT was supplied by Chang Chun Group under trade name PBT1100-211M with

Correspondence to: J.-W. Huang (jw.huang@msa.hinet.net).

a melt flow index (MFI) of 19.8 g/10 min (235°C × 2.16 kgf, ASTM D1238). Maleic anhydride grafted poly ethylene-octene (mPOE) with a MFI of 1.2 g/10 min (190°C × 2.16 kgf, ASTM D 1238), trade name: Fusabond® MN-493D was produced by Du Pont. POE with a MFI of 0.5 g/10 min (190°C × 2.16 kgf, ASTM D 1238) was also provided by Du Pont (Engage® 8150). All materials were used as received without purification.

Sample preparation

All materials were dried at 50°C in a vacuum oven for 6 h before compounding to eliminate extrusion bubbles. The low temperature (50°C) was unlikely to remove moisture completely, but it was selected after several trials to prevent bubble generation during the extrusion and not to adversely affect the material. PBT and 20 wt % POE (or mPOE) were compounded in a twin-screw extruder (L/D = 32, D = 40 mm, Continent Machinery Company, Model CM-MTE 32) at 280°C and 300 rpm to prepare polymer blend of PBT/POE (or PBT/mPOE). A mixture of 10 wt % POE and 10 wt % mPOE was blended with PBT in the extruder to prepare PBT/mPOE/POE. The rod extrudate was cooled in a water bath. As a base of comparison, the neat PBT was also passed trough the extruder at the same conditions.

Isothermal crystallization

Crystallization behavior of the blends was monitored with a DSC, Perkin–Elmer DSC-1. The DSC was calibrated using indium with samples weights of 8–10 mg. All operations were carried out in a nitrogen atmosphere. Before data collect on, the samples were heated to 280°C and held in the molten state for 5 min to eliminate the influence of thermal history. The samples melts were then subsequently quenched at a rate of 100°C/min to reach the specific temperatures and kept at that temperature for 1 h. When the crystallization process had completed, the samples were heated to 280°C at a rate of 10°C/min to measure the melting temperatures.

Morphology

To characterize the morphology of the blends, the samples were fractured in liquid nitrogen and examined with SEC (HITACHI, S-3500).

Wide-angle X-ray diffraction

WAXD was carried out using a Philips XRG-3000 generator with Ni filtered CuKα radiation (λ = 1.54 Å) which operated at an applied voltage of 30 kV and a current of 30 mA. The patterns were recorded at a scanning rate of 1°/min over an angular range of 10°–40°.

RESULTS AND DISCUSSION

Morphology of the PBT blends

Morphology is an important factor in determining the physical properties of the polymer blends. Figure 1 shows the scanning electron microscopy (SEM) micrographs of the fractured surface roughly normal to the extrusion direction. From Figure 1(a), it is clearly visible that POE particles were dispersed in the PBT matrix. When the components have different melt viscosities, the morphology of the blends depends on whether the minor component has a lower viscosity or a higher viscosity. If the minor component has a lower viscosity than the major one, the minor component will be finely dispersed.[12,13] The immiscibility of the two components resulted in phase segregation, where the minor phase was dispersed in large spherical domains and the dispersion was poor. As can be seen when Figure 1(a,b) are compared, the size of dispersed phase clearly decreased with the addition of mPOE. The decrease was from ca. 6–8 μm (PBT/POE) to ca. 2–4 μm (PBT/mPOE/POE). This decrease in size with the mPOE addition indicates that compatibility has been improved. Figure 1(c) shows the homogeneous character of the morphology in PBT/mPOE blend, where the mPOE phase was hardly distinguishable from the PBT matrix and the size of dispersed phase was <1 μm. This decrease in the particle size may be due to improved dispersibility attributable to reactions of the anhydride groups in mPOE and the OH in PBT at the interface.[14,15] The change in MFI is used as an indirect evidence for reaction in the melt.[16] The MFI of neat PBT, PBT/POE, PBT/mPOE/POE and PBT/mPOE are respectively 19.8, 19.4, 18.3, and 16.1. The MFI reduced in the presence of mPOE indicative of a reaction taking place at interface between PBT and POE.[16]

Wide-angle X-ray measurements

As shown in Figure 2 and Table I, the characteristic X-ray peaks for pure PBT were observed at the scattering angles 2θ of ca. 16.0, 17.2, 20.6, 23.3, 25.2, 29.3, and 31.1°, which correspond to the reflections from the $(0\bar{1}1)$, (010), $(\bar{1}11)$, (100), $(1\bar{1}1)$, (101), and $(\bar{1}\bar{1}1)$ planes, respectively.[17] The characteristic peaks of PBT/POE, PBT/mPOE/POE, and PBT/mPOE blends were similar to those of neat PBT. There were no new characteristic peaks appearing in the X-ray patterns of the blends indicating that the blending has no obvious effect upon the PBT crystal structure. Slight increase in d-spacings was observed with the

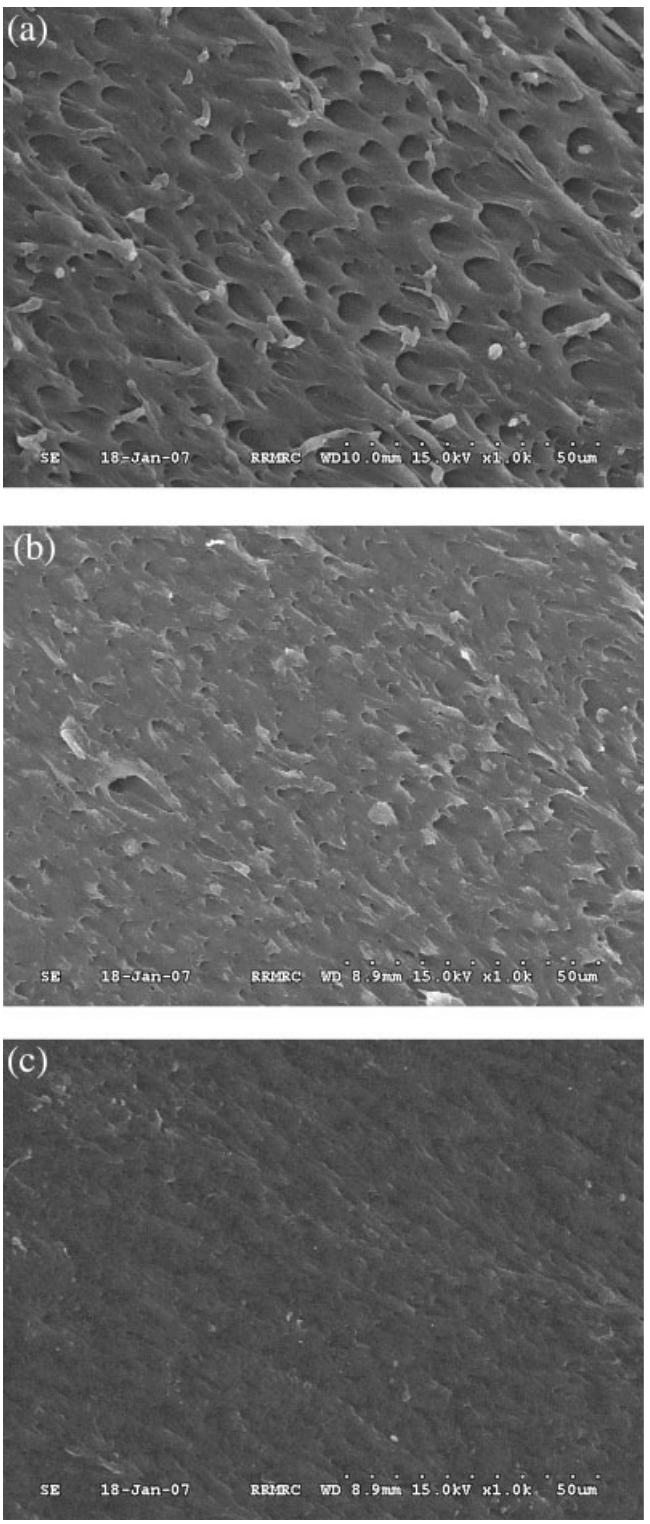

Figure 1 SEM micrograph of PBT/POE, PBT/mPOE/POE, and PBT/mPOE blends. (a) PBT/POE; (b) PBT/mPOE/POE; (c) PBT/mPOE.

addition of POE or mPOE. An increase in d-spacing can be explained by a decrease in the crystal sizes in the crystallographic directions according to Scherrer equation.[18] The well dispersed phases with smaller size would induce more nuclei, and higher nucleation density would induce smaller crystal. The size of dispersed phase decreased with increasing content of mPOE and induced much more nuclei to crystallize to form smaller crystal.

Melting behavior

Figure 3 exhibits the first DSC scans of PBT, PBT/POE, PBT/mPOE/POE, and PBT/mPOE that were quenched in water after blending in an extruder and some crystallization characteristics were listed in Table II. The crystallinity of the PBT is calculated according to the following relation:

$$\text{Crystallinity} = \frac{\Delta H_m}{w\,\Delta H_m^{\circ}} \tag{1}$$

where ΔH_m is the measured heat of fusion for the sample, and ΔH_m° is the heat of fusion for a 100% crystalline PBT, w is the mass fraction of PBT in the blend. According to previous studies, the heat of fusion of 100% crystalline PBT is 85.75 J/g.[19] Melting temperature (T_m), heat of fusion (ΔH_m) and crystallinity of PBT in all samples were not significantly affected by the presence of POE or mPOE. It indicated that the presence of elastic phase did not significantly change the melting process of PBT, as was previously seen in PBT/POE blends.[20]

However, the DSC scans of samples isothermally crystallized at different crystallization temperature (T_c), which were quenched from 553 K displayed two endotherms (T_{mI} and T_{mII}), as shown in Figure 4(a). These two melting endotherms have two possible origins: one is the melting of crystals with different morphologies[21,22]; the other come from

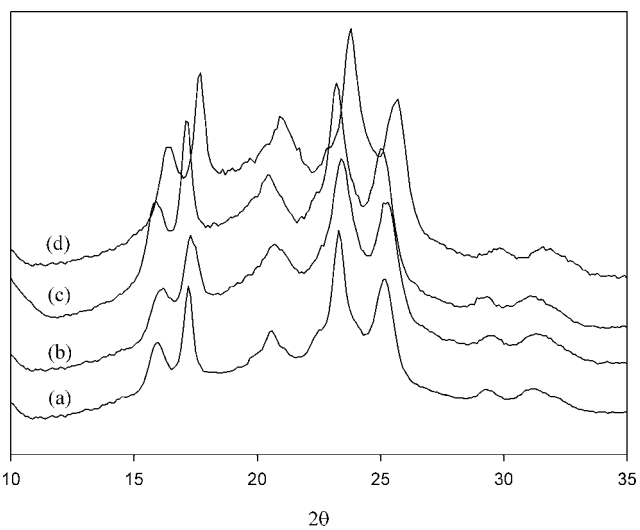

Figure 2 WAXD patterns of PBT, PBT/POE, PBT/mPOE/POE, and PBT/mPOE blends. (a) PBT; (b) PBT/POE; (c) PBT/mPOE/POE; (d) PBT/mPOE.

TABLE I
Peak Positions (as equivalent Bragg spacings d) for PBT, PBT/POE, PBT/mPOE/POE, and PBT/mPOE

Sample	Angle (2θ)	d-spacing (Å)	*hkl*
PBT	16.0	5.40	$(0\bar{1}1)$
	17.2	5.03	(010)
	20.6	4.21	$(\bar{1}11)$
	23.3	3.72	(100)
	25.2	3.45	$(1\bar{1}1)$
	29.3	2.97	(101)
	31.1	2.81	$(\bar{1}\bar{1}1)$
PBT/POE	16.2	5.34	$(1\bar{1}1)$
	17.3	5.00	(010)
	20.7	4.19	$(\bar{1}11)$
	23.4	3.71	(100)
	25.3	3.43	$(1\bar{1}1)$
	29.4	2.96	(101)
	31.3	2.79	$(\bar{1}\bar{1}1)$
PBT/mPOE/POE	16.2	5.34	$(1\bar{1}1)$
	17.4	4.97	(010)
	20.8	4.17	$(\bar{1}11)$
	23.2	3.74	(100)
	25.4	3.42	$(1\bar{1}1)$
	29.2	2.98	(101)
	31.5	2.77	$(\bar{1}\bar{1}1)$
PBT/mPOE	16.5	5.24	$(1\bar{1}1)$
	17.7	4.89	(010)
	20.9	4.15	$(\bar{1}11)$
	23.8	3.65	(100)
	25.7	3.38	$(1\bar{1}1)$
	29.8	2.92	(101)
	31.6	2.76	$(\bar{1}\bar{1}1)$

crystals with a less degree of perfection, which partially melt and recrystallize during DSC scans to yield more perfect crystals.[23,24] WAXD of all samples exhibited similar patterns as shown in Figure 2 suggesting that there was no additional phases as a resulted in the two melting peaks. The T_{mI} peak should be associated with the fusion of the crystals grown by normal primary crystallization and T_{mII} was the melting peak of the most perfect crystals after reorganization during the heating process in DSC measurement.[25]

The position of T_{mI} was influenced by the crystallization temperature for all samples. The position shifted to a higher temperature range and the magnitude of T_{mI} increased with the increase in crystallization temperature. But for T_{mII}, their positions remained almost unchanged and their intensity decreased when the crystallization temperature was increased. It indicated that the higher the crystallization temperature, the more perfect the crystals grown in normal primary crystallization.[25–27]

For a specific crystallization temperature, the T_{mI} shifted to a lower temperature and the intensity ratio of peak T_{mI} to peak T_{mII} decreased with the mPOE content in the PBT blend, as shown in Figure 4(b). It indicated that the addition of mPOE lowered the degree of perfection of the crystals grown in normal primary crystallization, and there was more recrystallization growth during DSC scan in PBT blend containing more dispersed second phases. Similar results have also been observed in PBT/Vectra blends.[27]

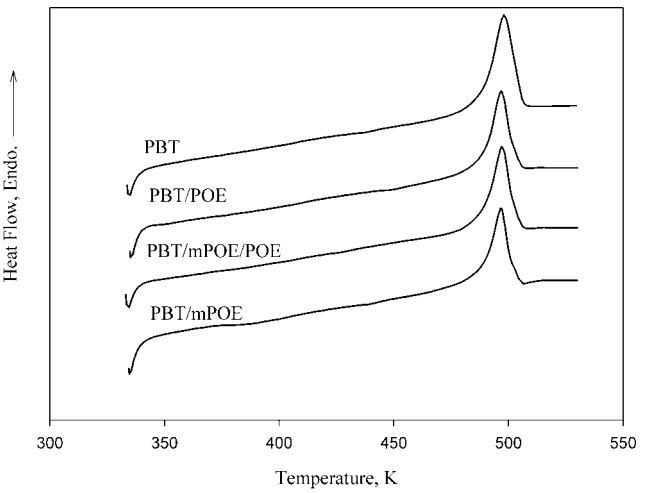

Figure 3 First DSC heating scan of PBT, PBT/POE, PBT/mPOE/POE, and PBT/mPOE which were quenched in water after blending in an extruder (heating rate 10 K/min).

Equilibrium melting temperature

The equilibrium melting temperature (ΔT_m^o) of a polymer is defined as the melting temperature of an infinite stack of extended chain crystals, large in directions perpendicular to the chain axis and where the chain ends have established an equilibrium state of pairing. The equilibrium temperature is a true reflection of a microstructure and the morphology of a blend, and it is the reference temperature from which the driving force for crystallization is measured.[28–30]

Hoffman–Weeks relation[31] has been extensively accepted to estimate the equilibrium melting temperature (ΔT_m^o), which can be determined by extrapolation of T_m versus T_c to $T_m = T_c$ (called linear H-W; LHW):

$$T_m' = T_m^{oLHW}\left(1 - \frac{1}{\gamma^{LHW}}\right) + \frac{T_c}{\gamma^{LHW}} \qquad (2)$$

The thickening coefficient $\gamma^{LHW} = l/l^*$, where l and l^* are the lamellar thickness at the time of melt-

TABLE II
DSC First Scan Data of PBT, PBT/POE, PBT/mPOE/POE, and PBT/mPOE

	PBT	PBT/POE	PBT/mPOE/POE	PBT/mPOE
T_m (K)	498	497	497	497
ΔH_m (J/g)	53.7	52.3	54.8	51.1
Crystallinity	62.6%	60.9%	63.8%	59.6%

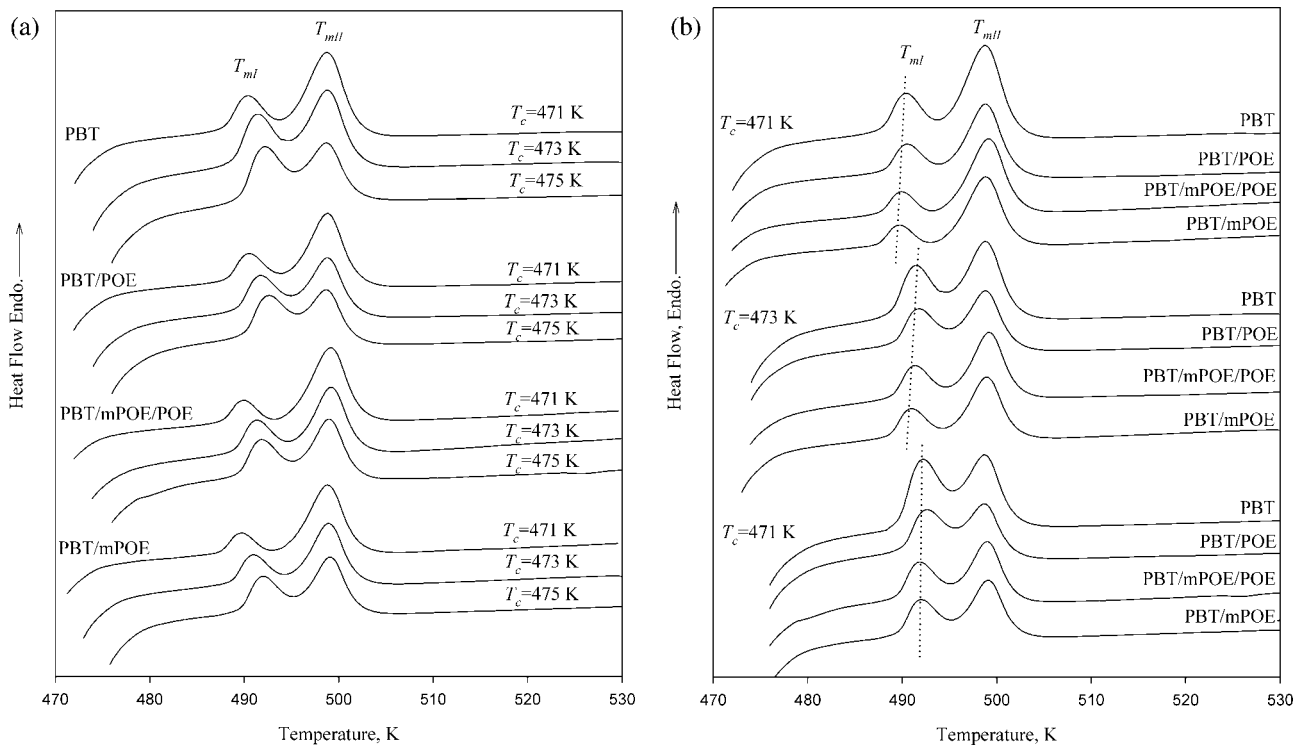

Figure 4 (a) Melting curves of PBT, PBT/POE, PBT/mPOE/POE, and PBT/mPOE after crystallization at different temperatures. (b) Comparisons of different samples isothermally crystallized at a specific temperature.

ing and the thickness of the critical nucleus at T_c, respectively. LHW plots were also shown in Figure 5(a), which indicated that T_m^{oLHW} for PBT, PBT/POE, PBT/mPOE/POE, and PBT/mPOE were, respectively, 509.4, 511.1, 523.6, and 499.9 K. The results of T_m^{oLHW} and γ^{LHW} were also tabulated in Table III. LHW analysis gave γ^{LHW} values of 1.81, 1.79, 1.62, and 2.96, respectively for PBT, PBT/POE, PBT/mPOE/POE, and PBT/mPOE, which were physically meaningless as it would imply rapid and significant thickening of polymer lamellae at very short time after their formation.

Alamo et al.[32] have explained the nonlinearity in the observed T_m and T_c. l^* should be dependent on the degree of undercooling ($\Delta T = T_m - T_c$) and $l^* = C_1/\Delta T + C_2$, where C_1 and C_2 are constant. But C_2 is always ignored in LHW. Marand et al.[33] proposed the following equation (nonlinear H-W; NLHW) to improve the linear Hoffman–Weeks relation:

$$M = \gamma^{NLHW}\left(\frac{\sigma_e^l}{\sigma_{em}}\right)(X + a) \tag{3}$$

$$M = \frac{T_m^{oNLHW}}{T_m^{oNLHW} - T_m} \tag{3a}$$

$$X = \frac{T_m^{oNLHW}}{T_m^{oNLHW} - T_c} \tag{3b}$$

$$a = \frac{\Delta H_f C_2}{2\sigma_e^l} \tag{3c}$$

where T_m^{oNLHW} is the equilibrium melting temperature for nonlinear Hoffman–Weeks equation, γ^{NLHW} is the thickening coefficient, σ_e^l is the interfacial energy associated with the basal plane of the mature crystallite, σ_{em} is the fold surface free energy associated with a nucleus of critical size including the extra lateral surface energy due to fold protrusion and the mixing entropy associated with stems of different lengths and ΔH_f is the heat of fusion of crystal. σ_e^l is assumed to be equal to σ_{em} in most cases.[33] According to eq. (3), γ^{NLHW} was the slope of the linear relation of M versus X for a specified T_m^{oNLHW} value, and a value [eq. (3c)] was the y-intercept. Once the T_m^{oNLHW} was selected, values of γ^{NLHW} and a could be estimated by a linear regression. The ''true'' equilibrium melting temperature (T_m^{oNLHW}) by this method was found when $\gamma^{NLHW} = 1$. The T_m^{oNLHW} of neat PBT, PBT/POE and PBT/mPOE were listed in Table III and the regression of the NLHW plot were also shown in Figure 5(b). There was apparent difference between LHW and NLHW with the NLHW estimate being higher in all samples.

Thermodynamics dictates that the addition of a miscible amorphous polymer results in the suppression of the chemical potential and melting point of a

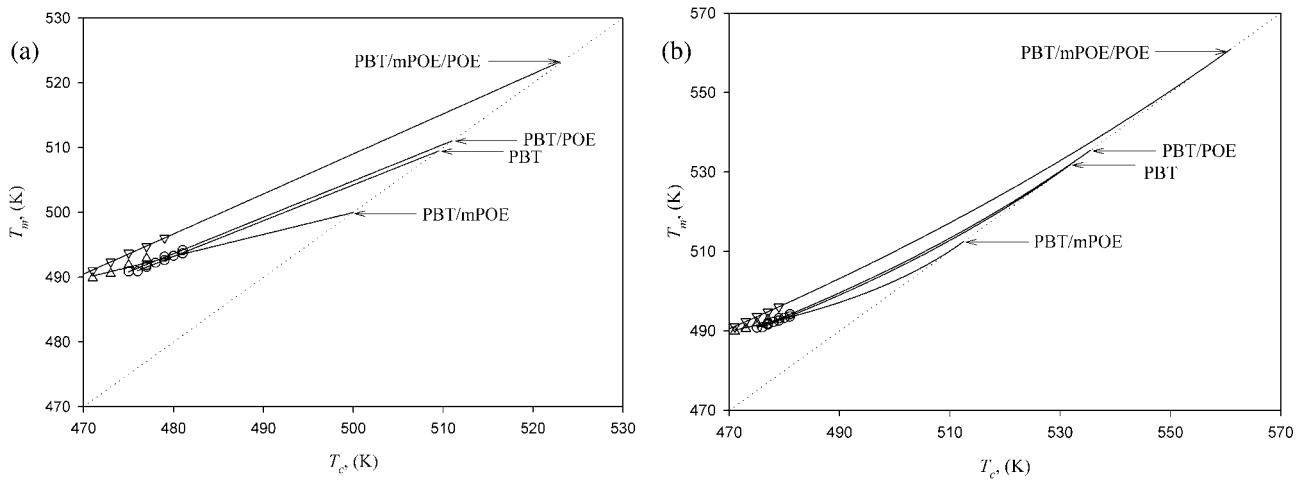

Figure 5 Equilibrium melting temperature estimated from (a) LHW and (b) NLHW.

crystallizable polymer. The equilibrium melting temperature of PBT/mPOE was lower, and PBT/POE was higher, than that of neat PBT. It indicated that mPOE had better compatibility with PBT.

Isothermal crystallization kinetics

Figures 6 shows the representative exothermic traces for PBT/mPOE isothermally crystallized at different temperatures. A sample crystallized at higher temperature required longer time to complete the crystallization process. The fraction of crystallinity, X_t, was calculated as the ratio of the exothermic peak areas at time t and infinite time:[34–36]

$$X_t = \frac{\int_0^t \left(\frac{dH_c}{dt}\right)dt}{\int_0^\infty \left(\frac{dH_c}{dt}\right)dt} \quad (4)$$

where dH_c is the enthalpy of crystallization released during an infinitesimal time interval dt. Figures 7 shows a typical relation between relative crystallinity (X_t) and time for PBT/mPOE, from which can be found half-time of crystallization $t_{1/2}$ defined as the time required to reach half of the final crystallinity ($X_t = 0.5$). In general, $t_{1/2}$ or $1/t_{1/2}$ is taken as a measure of the overall rate of crystallization of a polymer. As shown in Figure 8, $1/t_{1/2}$ of PBT decreased with increasing temperature for all samples.

TABLE III
Equilibrium Melting Temperature of PBT, PBT/POE, PBT/mPOE/POE, and PBT/mPOE

Sample	LHW		NLHW	
	T_m^{oLHW} (K)	γ^{LHW}	T_m^{oLHW} (K)	γ^{LHW}
PBT	509.4	1.81	532.0	1.00
PBT/POE	511.1	1.78	535.8	1.00
PBT/mPOE/POE	523.6	1.62	561.5	1.00
PBT/mPOE	499.9	2.96	512.5	1.00

Avrami analysis

By assuming the relative crystallinity increased with an increase in the crystallization time t, the Avrami equation can be used to analyze the isothermal crystallization process of polymers:[37–39]

$$X_t = 1 - \exp(-(K_a t)^{n_a}) \quad (5)$$

where X_t is the relative crystallinity, t is crystallization time, K_a is the Avrami crystallization rate constant and n_a is the Avrami exponent. X_t can be calculated from eq. (1). Values of K_a and n_a were found by fitting experimental data of X_t to eq. (2) and the results were shown in Table IV.

Avrami exponent represents a parameter revealing the nucleation mechanism and growth dimension. The Avrami exponent was found to vary from 1 to 4, corresponding to various growth forms from rod-like to sphere-like. For PBT, PBT/POE, and PBT/

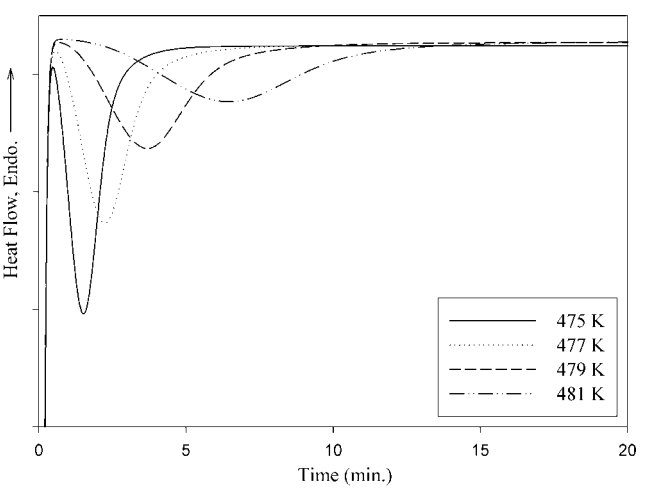

Figure 6 DSC isothermal measurement curves for PBT/mPOE blend.

TABLE IV
Avrami Kinetics Parameters

Sample	T_c (K)	n_a	K_a (min^{-1})	R^2
PBT	476	2.65	0.4374	0.9998
	477	2.58	0.3521	0.9998
	478	2.56	0.2737	0.9998
	479	2.47	0.2031	0.9999
	480	2.42	0.1504	0.9999
	481	2.43	0.1104	0.9999
PBT/POE	475	2.613	0.8013	0.9999
	477	2.52	0.4809	0.9996
	479	2.47	0.2611	0.9979
	481	2.72	0.1445	0.9987
PBT/mPOE/POE	471	2.79	0.4233	0.9999
	473	2.68	0.3118	0.9996
	475	2.41	0.2027	0.9985
	477	2.18	0.1193	0.9973
	479	2.46	0.0686	0.9984
PBT/mPOE	471	2.49	0.4839	0.9998
	473	2.64	0.3595	0.9998
	475	2.41	0.2079	0.9984
	477	2.59	0.1242	0.9998

mPOE samples, the n_a values observed in the Table I were between 2.4 and 2.8. No evident changes of the values of n_a with the addition of POE or mPOE was noticed. Therefore, it may be reasonable to consider that the addition of POE or mPOE did not affect the geometric dimension of PBT crystal growth. Wunderlich[40] has attributed an Avrami exponent of three to spherical structure resulting from instantaneous nucleation (that is, the number of nuclei reaches a steady state value rapidly after crystallization begins) and an exponent n_a between two and three to truncated spheres resulting from instantaneous nucleation with diffusion control. The Avarami model seemed to provide a good fit to experimental data from regression coefficients.

Although n_a may be considered as a constant with crystallization temperatures (T_c), K_a depends strongly on T_c. The isothermal rate constants, K_a, were also shown in the Table I as a function of T_c for three samples. This indicated that the values of K_a decreased with increasing T_c.

To reconstruct in regression analysis with the Avrami models is shown in Figure 7 for all four samples crystallized isothermally. It can be seen from Figure 7 that the Avrami model provided a good fit to the experimental data over the entire range of the crystallization.

At a specific T_c, ranking of both $1/t_{1/2}$ and K_a in Figure 8 and Table IV follow the order: PBT/POE > PBT > PBT/mPOE > PBT/mPOE/POE. However, crystallizability should be compared at the same degree of undercooling ($T_m^o - T_c$) for samples with different equilibrium melting temperatures since crystallization rate of a polymer depends strongly on undercooling. Undercooling, $1/t_{1/2}$, and

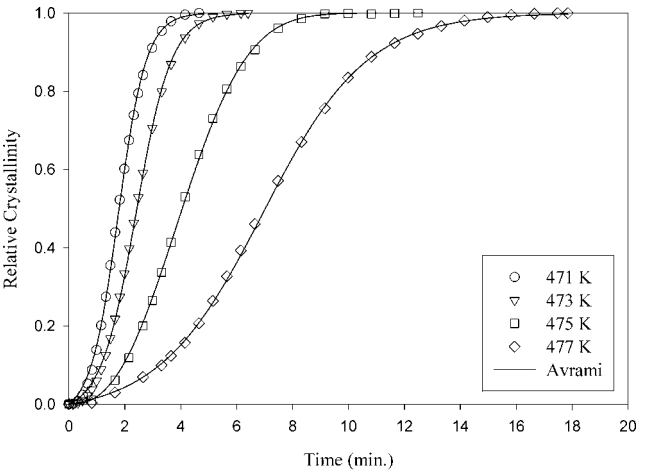

Figure 7 Relative crystallinity as a function of crystallization temperature from experimental data and Avrami model for PBT/mPOE blend.

rate constants based on the Avrami model were shown in Figure 9(a,b). All four samples showed similar trend that the crystallization rate constants increased with increasing undercooling indicating higher crystallization rate at greater undercooling. At a specific value of rate constant, PBT/mPOE needed to be imposed the lowest undercooling, followed by PBT, PBT/POE, and PBT/mPOE/POE; it indicated that the crystallization rate followed the order: PBT/mPOE > PBT > PBT/POE > PBT/mPOE/POE. Undercooling is an important factor to study crystallization behaviors because the parameter ensures that the systems being compared experienced the same thermal history.[40–42] Because of experimental limitations, only crystallization rate at low undercooling could be measured easily. A second component added to the blend would either act as a nucleating agent to increase crystallization

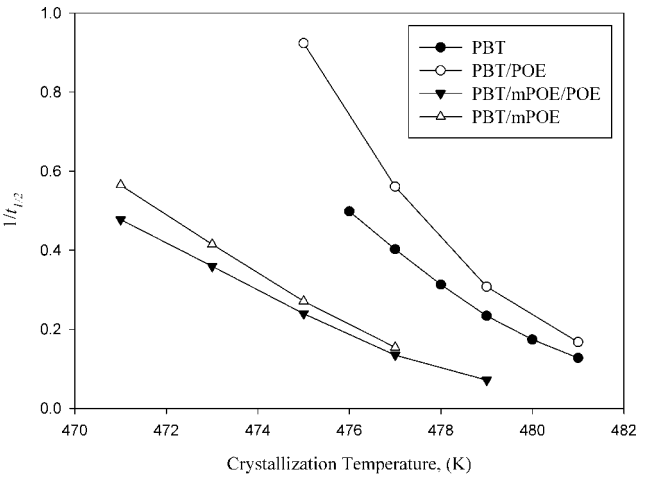

Figure 8 $1/t_{1/2}$ as a function of crystallization temperature.

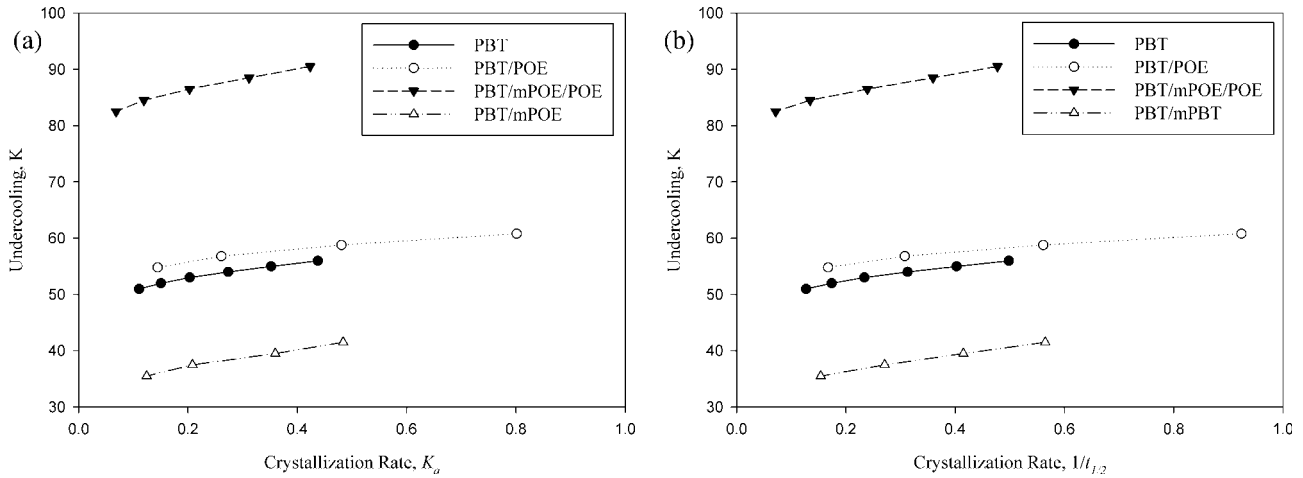

Figure 9 Relation of undercooling and rate constants evaluated from (a) Avrami model; (b) $1/t_{1/2}$.

rate or retard the molecular mobility to slow down the crystallization. The overall crystallization rate is governed by nucleation and diffusion.[43,44] Dispersion phases in PBT/mPOE/POE was smaller but more numerous than that in PBT/POE. These fine dispersions would hinder the crystallization by slowing down the diffusion of PBT chains and results in a lower crystallization rate. A well dispersed phases with smaller size (as in PBT/mPOE) would produce more nuclei and induce higher nucleation density to enhance crystallization. When the nucleation effect is over the hindrance, the crystallization rate is increased. Therefore, PBT in PBT/mPOE has highest crystallization rate. Similar phenomenon was also observed in polyethylene/ vermiculite composites.[44]

Temperature dependence of overall crystallization rate

Hoffman and Lauritzen[45] propose the following equation to include nucleation and growth phenomena for overall crystallization rate:

$$\psi(T_c) = \psi_0 \exp\left[\frac{-U^*}{R(T_c - T_\infty)} - \frac{K_g}{T_c(\Delta T)f}\right] \qquad (6)$$

where $\psi(T_c)$ is crystallization rate parameter and ψ_0 is a pre-exponential term; $U^* = 1500$ cal/mole is the diffusional activation energy for the transport of crystallizable segments at the liquid–solid interface; R is the gas constant; $T_\infty = T_g - 30\ K$ is the hypothetical temperature below which viscous flow ceases; T_g is glass transition temperature of PBT and had been studied by many researchers.[44–46] $T_g = 248$ K seems reasonable.[44,45] $\Delta T = T_m^o - T_c$; $f = 2T_c/(T_m^o + T_c)$ is a correction factor; K_g is the nucleation parameter which can be related to the product of lateral and folding surface free energy.

The crystallization rate parameter $\psi(T_c)$ could be considered proportional to $1/t_{1/2}$, eq. (6) can be rewritten as:

$$\frac{1}{t_{1/2}} = \psi_0 \exp\left[\frac{-U^*}{R(T_c - T_\infty)} - \frac{K_g}{T_c(\Delta T)f}\right] \qquad (7a)$$

or

$$\ln\left(\frac{1}{t_{1/2}}\right) + \frac{U^*}{R(T_c - T_\infty)} = \ln\psi_0 - \left(\frac{K_g}{T_c(\Delta T)f}\right) \qquad (7b)$$

Figure 10 shows the plot of eq. (7b) for PBT, PBT/POE, and PBT/mPOE by using $T_m^o = T_m^{oNLHW}$. The K_g and ψ_0 could be obtained from the slope and intercept of Figure 10 and the results were listed in Table V. Different values of T_m^o from LHW and nonlinear were also used to calculate K_g and ψ_0, and the results were listed in Table V for comparison. K_g of PBT in PBT/mPOE is lower than that of PBT suggesting that the well-dispersed fine mPOE phases can act as effective nucleating agents for PBT. On the other hand, the larger dispersed phases give rise to restrictions on PBT segment mobility and the K_g of PBT in PBT/POE and PBT/mPOE/POE are higher than that of PBT. The results were similar to polypropylene/epoxy blends.[47]

By taking the results of Table V ($T_m^o = T_m^{oNLHW}$) to eq. (7b), the undercooling ($T_m^{oNLHW} - T_c$) dependence of rate function ($1/t_{1/2}$) could be obtained as shown in Figure 11. The bell-shaped curve is attributed to the nucleation control effect at low undercooling (high crystallization temperature) and the diffusion control effect at high undercooling (low crystallization temperature). At low undercooling, finer mPOE dispersing phases act as nucleating agents for PBT to increase the crystallization rate. At high undercooling, the mPOE had good compatibility with PBT would increase melt viscosity and reduce mobility of

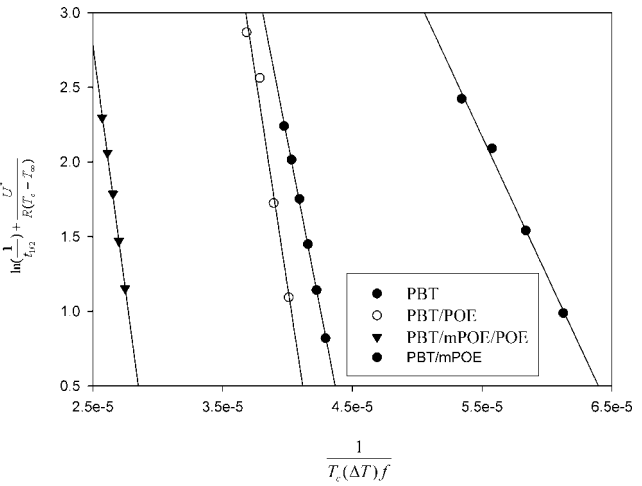

Figure 10 Plot of $\ln\left(\frac{1}{t_{1/2}}\right) + \frac{U^*}{R(T_c - T_\infty)}$ as a function of $\ln \psi_0 - \left(\frac{K_g}{T_c(\Delta T)f}\right)$.

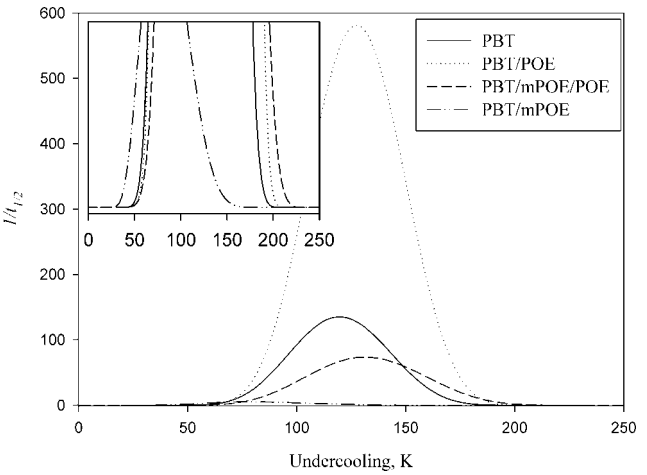

Figure 11 The fitted curves drawn through the data after eq. (7b) ($T_m^o = T_m^{oNLHW}$).

the polymer chains during crystallization. The trend of crystallization rate at lower undercooling is: PBT/mPOE > PBT > PBT/POE > PBT/mPOE/POE; it similar to the results obtained above.

CONCLUSIONS

SEM analysis on morphologies of PBT/POE and PBT/mPOE blends revealed improved compatibility between PBT and POE in the presence of maleic anhydride groups. The addition of POE or mPOE did not affect the melting behavior of PBT as samples quenched in water after blending in an extruder; on the other hand, the addition of POE or mPOE phase altered crystallization rate of the blends. Subsequent DSC scans of isothermally crystallized PBT and PBT blends exhibited two melting endotherms (T_{mI} and T_{mII}), respectively, which was due to the melt-recrystallization process during the DSC scans. Lower crystallization temperature and more dispersed second phases led to crystals with lower perfection in normal primary crystallization. The dispersed phases could hinder the crystallization by slowing down the diffusion of PBT chains; on the other hand, well dispersed phases with smaller size (as in PBT/mPOE) would enhance crystallization because of higher nucleation density. Ranking of the crystallization rate during experimental range was: PBT/mPOE > PBT > PBT/POE > PBT/mPOE/POE.

TABLE V
Nucleation Factor, K_g, for PBT, PBT/POE, PBT/mPOE/POE, and PBT/mPOE

Samples	T_m^o (K)	$K_g \times 10^{-5}$	R^2
PBT	T_m^{oLHW}, 509.4	1.39	0.9995
	T_m^{oNLHW}, 532.0	4.47	0.9978
PBT/POE	T_m^{oNLHW}, 511.1	1.73	0.9816
	T_m^{oLHW}, 535.8	5.69	0.9787
PBT/mPOE/POE	T_m^{oNLHW}, 523.6	1.81	0.9996
	T_m^{oLHW}, 561.5	6.51	0.9989
PBT/mPOE	T_m^{oNLHW}, 499.9	0.81	0.9967
	T_m^{oLHW}, 512.5	1.86	0.9949

References

1. Aróstegui, A.; Gaztelumedi, M.; Nazábal, J. Polymer 2001, 42, 9565.
2. Guerrica-Echevarria, G.; Eguiazabal, J. I.; Nazabal, J. Polym Eng Sci 2006, 46, 172.
3. Aróstegui, A.; Nazábal, J. Polym Eng Sci 2003, 43, 1691.
4. Hale, W.; Keskkula, H.; Paul, D. R. Polymer 1999, 40, 365.
5. Hale, W.; Keskkula, H.; Paul, D. R. Polymer 1999, 40, 3665.
6. Wang, H. X.; Zhang, H. X.; Wang, Z. G.; Jiang, B. Z. Polymer 1997, 38, 1569.
7. Vongpanish, P.; Bhowmick, A. K.; Inoue, T. Plast Rubber Comp Proc Appl 1994, 21, 109.
8. Aróstegui, A.; Nazábal, J. J Polym Sci Part B: Polym Phys 2003, 41, 2236.
9. Finelli, L.; Lotti, N.; Righetti, M. C.; Munari, A. J Appl Poly Sci 2001, 81, 3545.
10. Lotti, N.; Finelli, L.; Siracusa, V.; Munari, A.; Gazzano, M. Polymer 2002, 43, 4355.
11. Wang, Y.; Bhattacharya, M., Mano, J. F. J Polym Sci Part B: Polym Phys 2005, 43, 3077.
12. Runt, J.; Miley, D. M.; Zhang, X.; Gallagher, K. P.; McFeaters, K.; Fisburn, J. Macromolecules 1992, 25, 1929.
13. Palanivelu, K.; Sivaraman, P.; Reddy, M. D. Polym Testing 2002, 21, 345.
14. Grigoryeva, O. P.; Karger-Kocsis, J. Eur Polym J 2000, 36, 1419.
15. Loyens, W.; Groeninckx, G. Macromol Chem Phys 2002, 203, 1702.
16. Kim, C. H.; Cho, K. Y.; Park, J. K. Polymer 2001, 42, 5135.
17. Wang, B.; Li, Y. C.; Hanzlicek, J.; Cheng, S. Z. D.; Geil, P. H.; Grebowicz, J.; Ho, R. M. Polymer 2001, 42, 7171.
18. Vickers, M. In Scattering Methods in Polymer Science; Richards, R. W., Ed. Ellis Horwood: London, 1995; Chapter 5.
19. Yokouchi, M.; Sakakibara, Y.; Chantani, Y.; Tadokoro, H.; Tanaka, T.; Yoda, K. Macromolecules 1976, 9, 266.
20. Aróstegui, A.; Nazábal, J. Polymer 2003, 44, 239.

21. Roberts, R. C. Polymer 1969, 10, 113.
22. Roberts, R. C. Polymer 1969, 10, 117.
23. Nichols, M. E.; Robertson, R. E. J Polym Sci Part B: Polym Phys 1992, 30, 305.
24. Huang, J. M. J Polym Sci Part B: Polym Phys 2004, 42, 1694.
25. Liu, X.; Li, C.; Zhang, D.; Xiao, Y. J Polym Sci Part B: Polym Phys 2006, 44, 900.
26. Lai, W. C.; Liau, W. B.; Lin, T. T. Polymer 2004, 45, 3073.
27. Kalkar, A. K.; Deshpande, A. A. Polym Eng Sci 2001, 41, 1597.
28. Hoffman, J. D.; Davis, G. T.; Lauritzen, J. I. Treatise on Solid State Chemistry; Plenum Press: New York, 1976.
29. Hoffman, J. D.; Miller, R. L. Polymer 1997, 38, 3151.
30. Armitstead, K.; Goldbeck-Wood, G. Adv Polym Sci 1992, 100, 219.
31. Hoffman, J. D.; Weeks, J. J. J Res Nat Bur Stand 1962A, 66, 13.
32. Alamo, R. G.; Viers, B. D.; Mandelkern, L. Macromolecules 1995, 28, 3205.
33. Marand, H.; Xu J.; Srinivas, S. Macromolecules 1998, 31, 8219.
34. Hay, J. N.; Sabir, M. Polymer 1969, 10, 203.
35. Hay, J. N.; Fitzgerald, P. A.; Wiles M. Polymer 1976, 17, 1015.
36. Gao, Q.; Scheinbeim, J. Polym J 2003, 35, 345.
37. Avrami, M. J. Chem Phys 1939, 7, 1103.
38. Avrami, M. J. Chem Phys 1940, 8, 212.
39. Avrami, M. J. Chem Phys 1941, 9, 177.
40. Wunderlich, B. Macromolecular Physics; Academic Press: New York, 1976.
41. Causin, V.; Marega, C.; Marigo, A.; Valentini, L.; Kenny, J. M. Macromolecules 2005, 38, 409.
42. Di Lorenzo, M. L.; Silvestre, C. Prog Polym Sci 1999, 24, 917.
43. Bai, H.; Zhang, Y.; Zhang, Y.; Zhang, X.; Zhou, W. J Appl Poly Sci 2006, 101, 1295.
44. Tjong, S. C.; Bao, S. P. J Polym Sci Part B: Polym Phys 2005, 43, 253.
45. Hoffman, J. D.; Frolen, L. J.; Ross G. S.; Lauritzen, J. I. J Res NBS 1975, 79A, 671.
46. Cheng, S. Z. D.; Pan, R.; Wunderlich, B. Makromol Chem 1988, 189, 2443.
47. Farrow, G.; McIntosh, J.; Ward, I. M. Makromol Chem 1960, 38, 147.